Exploring Electronic and Structural Properties of Titanium-Doped Chlorapatite: A Theoretical and Experimental Investigation

Serhat Keser [1, *], Tankut Ates [2], Niyazi Bulut [3], Omer Kaygili [3]

[1]*Department of Chemical Technology, EOSB Vocational School, Firat University, 23119, Elazig, Türkiye*
[2]*Department of Engineering Basic Sciences, Faculty of Engineering and Natural Sciences, Malatya Turgut Özal University, Battalgazi, Malatya, Türkiye*
[3]*Department of Physics, Faculty of Science, Firat University, 23119, Elazig, Türkiye*
Corresponding author: Serhat Keser E-mail: serhatkeser@gmail.com

ABSTRACT

The apatite family stands as a pivotal class of inorganic compounds with diverse elemental components, playing a crucial role in biological, environmental, and geological contexts. Among these, chlorapatite (ClAp) emerges as a significant member, featuring a hexagonal structure with the space group $P6_3/m$. In this theoretical study, we delve into the unexplored realm of Ti-doped ClAp structures, investigating their electronic and structural characteristics for the first time. Motivated by the potential impact of titanium (Ti) doping on electronic and optical properties, we employ density functional theory (DFT) principles to perform band structure calculations. The electronic band structure is explored comprehensively, shedding light on the energy distribution for electrons as a function of momentum. Our calculations reveal that un-doped ClAp exhibits an insulating nature, as indicated by a calculated band gap of approximately 4.947 eV. The theoretical volume parameter closely matches experimental observations, validating the reliability of our computational model. Introducing Ti as a dopant in 1.2TiClAp results in a discernible increase in the band gap to approximately 5.339 eV. The theoretical volume parameter exhibits excellent agreement with experimental data, emphasizing the precision of our calculations. For 2.4TiClAp, the band gap remains stable at around 5.344 eV, while the theoretical volume parameter stands at 0.5260 nm^3. Our systematic exploration of Ti-doped ClAp underscores the tunability of electronic properties, signifying potential applications across diverse fields. The reliability of theoretical calculations is further affirmed by the consistent alignment with experimental parameters. These findings contribute significantly to our fundamental understanding of Ti-doped ClAp, providing crucial insights for material design and optimization. Ongoing collaborative efforts between theoretical and experimental approaches are essential for a comprehensive assessment of these complex materials.

ARTICLE INFO

1. Introduction

The apatite family is an important class of inorganic compounds and includes a lot of compounds with different elemental components. Apatites are naturally occurring minerals widely distributed in igneous rocks [1]. Apatites have the general formula of the $M_{10}(PO_4)_6X_2$ or $M_5(PO_4)_3X$ and have significant biological, environmental and geological importance [2-4]. Here, M = a divalent metal ion such as Ca, Sr, Ba, Pb, and X = OH^-, Cl^-, F^-. There are varieties where X is F^- (fluorapatite, FAp, $Ca_5(PO_4)_3F$), OH^- (hydroxyapatite, HAp, $Ca_5(PO_4)_3(OH)$) and Cl^- (chlorapatite, ClAp, $Ca_5(PO_4)_3Cl$) [1-5].

Chlorapatite $Ca_5(PO_4)_3Cl$ (ClAp) is an important compound of the apatite family, which has a hexagonal structure with the space group $P6_3/m$ [1-3,6]. M atoms are located in two different places, MI and MII. The former is surrounded by 9 oxygen atoms, while the latter is surrounded by two Cl^- ions and 6 oxygen atoms of the PO_4^{3-} network. Oxygen atoms are surrounded by P as a tetragonal structure like PO_4. In the ClAp structure, since the CaI region is smaller than the CaII region, large ions such as trivalent rare earth ions easily settle in the CaII regions [7].

The properties of ClAp nanocrystals can be improved by controlling parameters such as size, distribution and structural morphology [8]. Synthetic ClAp nanoparticles can be produced by a number of techniques categorized as dry methods, wet methods, high temperature treatment and their combination procedures [8]. These methods are classical solid state reaction [4,7,9], mechanochemical [8], precipitation [7,8], pyrolysis [8,9], hydrothermal and aqueous colloidal [7,9,10], microwave [9,10], sol-gel [9], solution burning [10], and wet chemical [8,11].

The doping processes are carried out to improve the required properties of the produced materials. In the literature, the use of Eu [10-12], Ta [13], Zr [14], Ce [15], Tb [16], Sm [17] and carbonate [18] as the dopants for the ClAp have been reported.

Zhang et al. [16] synthesized Eu^{3+}/Tb^{3+} co-doped ClAp by conventional solid-state synthesis method. Kim et al. [17] investigated the photoluminescence properties of Eu^{3+} and Sm^{3+} doped ClAp at different sintering temperatures.

In the present study, we investigated Ti-doped ClAp structures for the first time, as well as we know.

2. Materials and methods

Calcium chloride (CC), titanium(IV) butoxide (TB) and diammonium hydrogen phosphate (DAP) were used as the starting chemicals for the synthesis. For each sample, 100 mL of 50-x mmol of CC and x mmol TB solution and 100 mL of 30 mmol DAP solution were prepared in different flasks. Where x was 0, 0.6, and 1.2. The DAP solution was poured into the CC and TB solution put into a beaker of 400 mL, the new mixture was stirred at 100 °C for 120 min, and then put into an oven at 300 °C for 120 min. The as-dried powders were calcined in an electrical furnace at 825 °C for 2 h.

X-ray diffraction analyses were carried out using a Rigaku Rad B-DMAX II diffractometer. Fourier transform infrared (FTIR) measurements were done using a PerkinElmer Spectrum One spectrophotometer using the KBr method. For the morphological observations, a ZEISS EVO 50 scanning electron microscope was used.

3. Theoretical Foundation of Band Structure Calculations

The electronic band structure plays a pivotal role in unraveling the electronic and optical characteristics of materials. Within the framework of chlorapatite (ClAp) structures, a comprehensive understanding of the electronic band structure becomes imperative, particularly when introducing different elements through doping. This theoretical segment delves into the fundamentals of band structure calculations and their application in scrutinizing Ti-doped ClAp, utilizing the CASTEP software [19].

3.1 Electronic Band Structure: A Comprehensive Overview

The electronic band structure serves as a depiction of the distribution of energy levels for electrons within a material relative to their momentum. It provides valuable insights into the electrical conductivity, optical behaviors, and other electronic features of the material. The band structure is conventionally computed by resolving the Schrödinger equation for electrons within a periodic crystal lattice.

3.2 Principles Governing Band Structure Calculations

The calculation of the electronic band structure of materials commonly employs density functional theory (DFT). DFT, a quantum mechanical approach, models the electronic structure of a material based on the spatial distribution of its electron density. The CASTEP software, grounded in DFT principles, stands as a widely utilized tool for such intricate calculations.

In DFT, the total energy of the system is formulated as a functional of the electron density. The Kohn-Sham equations are then solved iteratively, leading to the determination of electronic wave functions and eigenvalues. These eigenvalues, in turn, enable the derivation of the electronic band structure.

3.3 Application to Ti-Doped ClAp

In the context of Ti-doped ClAp, the introduction of titanium (Ti) as a dopant induces alterations in the electronic structure, potentially resulting in modified electronic and optical properties. The CASTEP software facilitates the modeling of the electronic band structure of Ti-doped ClAp, integrating crystal structure information and specifying dopant concentrations. The calculations involve establishing the unit cell, defining lattice parameters, and stipulating electronic and geometric convergence criteria. The software employs numerical methods and algorithms to iteratively solve the Kohn-Sham equations, furnishing crucial information on energy bands, band gaps, and electronic density of states.

3.4 Significance of Band Structure in Ti-Doped ClAp

A profound comprehension of the electronic band structure of Ti-doped ClAp proves pivotal in predicting its conductivity, optical absorption, and other electronic properties. Theoretical band structure calculations serve as guiding principles for experimental endeavors, offering insights into the potential impact of Ti doping on the material's overall performance.

To summarize, the theoretical calculations of the electronic band structure utilizing the CASTEP software present a potent tool for delving into the electronic properties of Ti-doped ClAp. These insights, in turn, contribute to the strategic design and optimization of ClAp-based materials across diverse applications, ranging from optoelectronics to catalysis.

4. Results

4.1. Theoretical results

The as-optimized structure for the un-doped ClAp structure is drawn with the VESTA software [20] in Fig. 1. Figs. 2, 3 and 4 show the band structure and DOS plots for ClAp, 1.2TiClAp and 2.4TiClAp structures, respectively. The as-obtained theoretical results related to the cell parameters for each structure are given in Table 1. The

comprehensive insights gained from theoretical calculations illuminate the intricate electronic and structural attributes of chlorapatite (ClAp) and its titanium-doped derivatives, 1.2TiClAp and 2.4TiClAp. In the case of un-doped ClAp, the calculated band gap of approximately 4.947 eV aligns coherently with its insulating nature, as supported by the experimental volume parameter of 0.5638 nm^3, which closely corresponds to the theoretical value of 0.5539 nm^3. The introduction of 1.2at.% titanium doping in 1.2TiClAp brings about a discernible elevation in the band gap to approximately 5.339 eV. The precision of the theoretical model is underscored by the close agreement between the theoretical volume parameter (0.5538 nm^3) and the experimentally observed value (0.5484 nm^3). Transitioning to 2.4TiClAp, the band gap remains relatively stable at approximately 5.344 eV, while the theoretical volume parameter is around 0.5260 nm^3, its experimental value is 0.5430 nm^3. The systematic increase in band gaps with escalating titanium concentrations emphasizes the tunability of electronic properties in titanium-doped chlorapatite, showcasing its potential for tailored applications across various fields. The reliability of theoretical calculations is reinforced by the consistent alignment between theoretical and experimental volume parameters, instilling confidence in the accuracy of the computational predictions. These results significantly contribute to the foundational comprehension of the electronic behavior of Ti-doped ClAp, providing invaluable insights for the refinement and optimization of material design in practical applications.

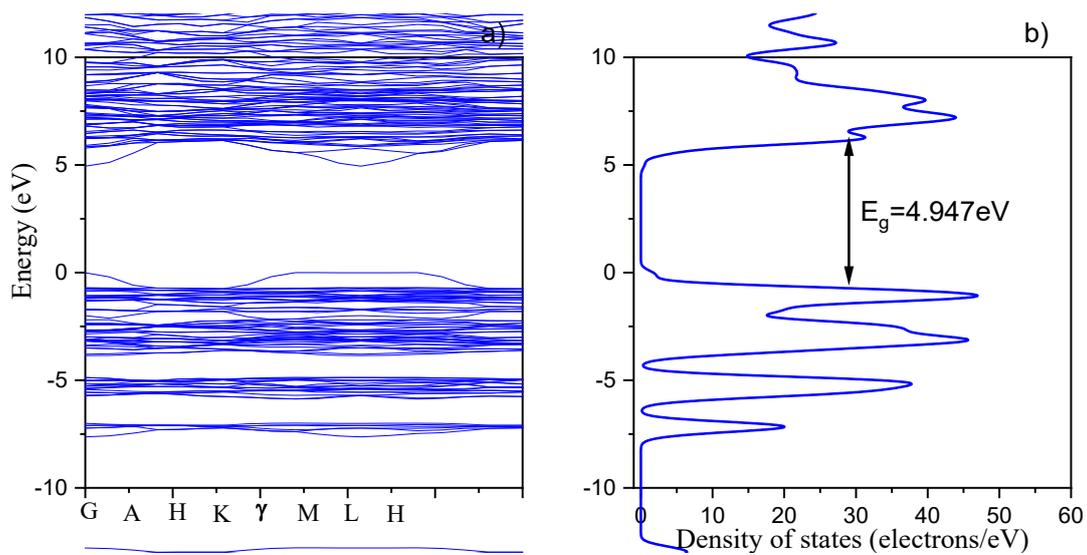**Figure 1.** The as-modeled structure for the ClAp structure

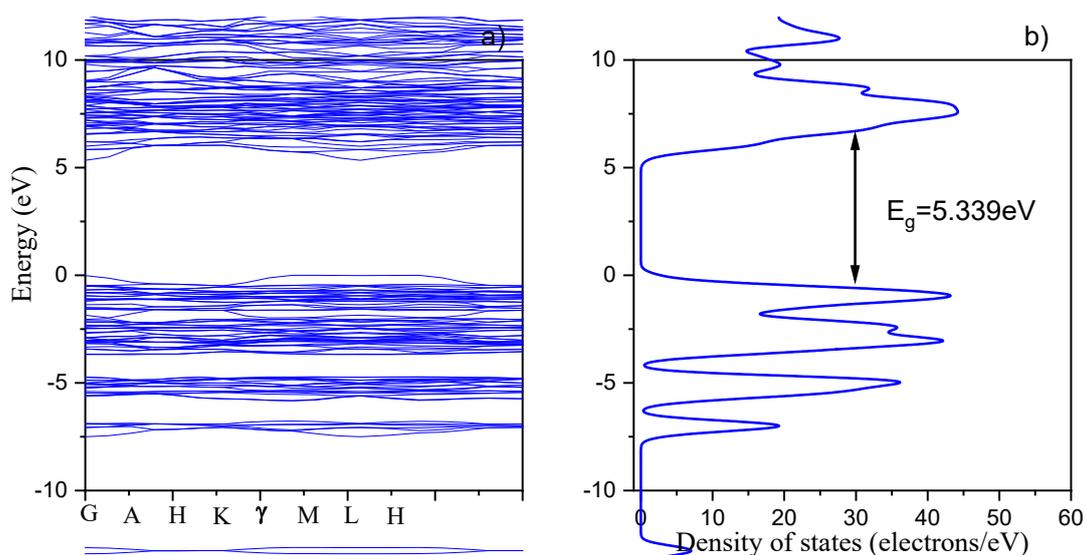**Figure 2. a)** Band structure and **b)** DOS for the ClAp structure

Figure 3. a) Band structure and **b)** DOS for the 1.2TiClAp structure
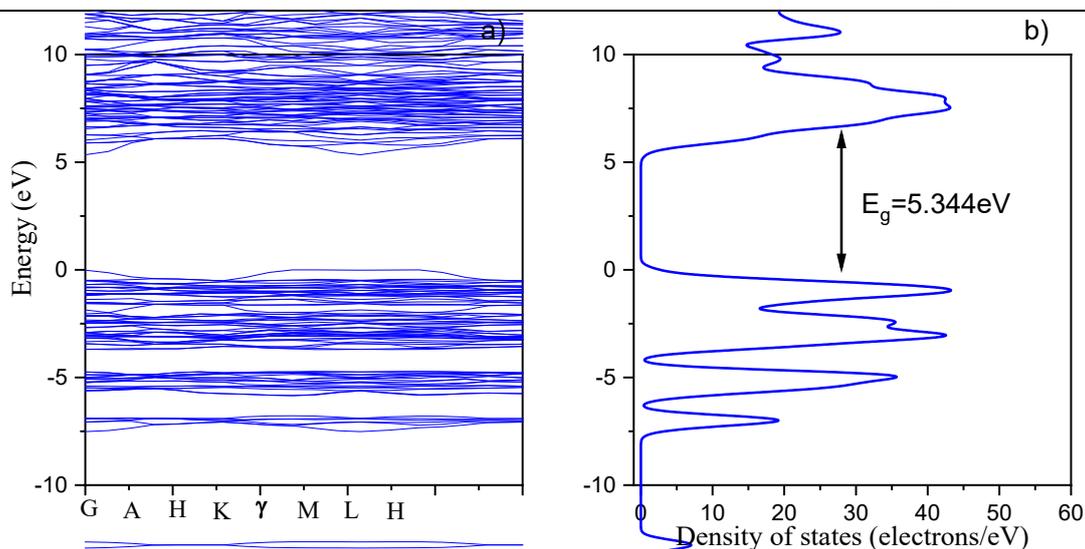
Figure 4. a) Band structure and **b)** DOS for the 2.4TiClAp structure

Table 1. A comparison between theoretical and experimental results

		a (nm)	c (nm)	V (nm)^3
Theoretical	ClAp	0.9814	0.6641	0.5539
	1.2Ti-ClAp	0.9817	0.6635	0.5538
	2.4Ti-ClAp	0.9397	0.6878	0.5260
Experimental	ClAp	0.9646	0.6997	0.5638
	1.2Ti-ClAp	0.9622	0.6840	0.5484
	2.4Ti-ClAp	0.9615	0.6782	0.5430

4.2. Experimental results

4.2.1. XRD results

Fig. 5 illustrates the powder XRD analysis results of the samples. For all the samples, the as-obtained patterns are in good agreement with the reported one for the ClAp (JCPDS pdf no 84-1999) having a hexagonal crystal structure. The as-calculated lattice parameters from the XRD data for each sample are tabulated and compared to the theoretical ones in Table 1. The experimental results showed a continuous decrease in the lattice parameters and volume of the unit cell. As known, Ca^{2+} has an ionic radius of 0.099 nm and Ti^{4+} has 0.068 nm [21]. The occupation of an ion with larger radius by the smaller one causes shrinkage in the lattice. The crystallite size (D) was estimated using the well-known Scherrer equation [22]. The D values were computed to be 35.66, 31.22, and 35.20 nm for the ClAp, 1.2TiClAp and 2.4TiClAp, respectively. Compared to the un-doped sample, it was found that Ti-doped samples have lower crystallite sizes.
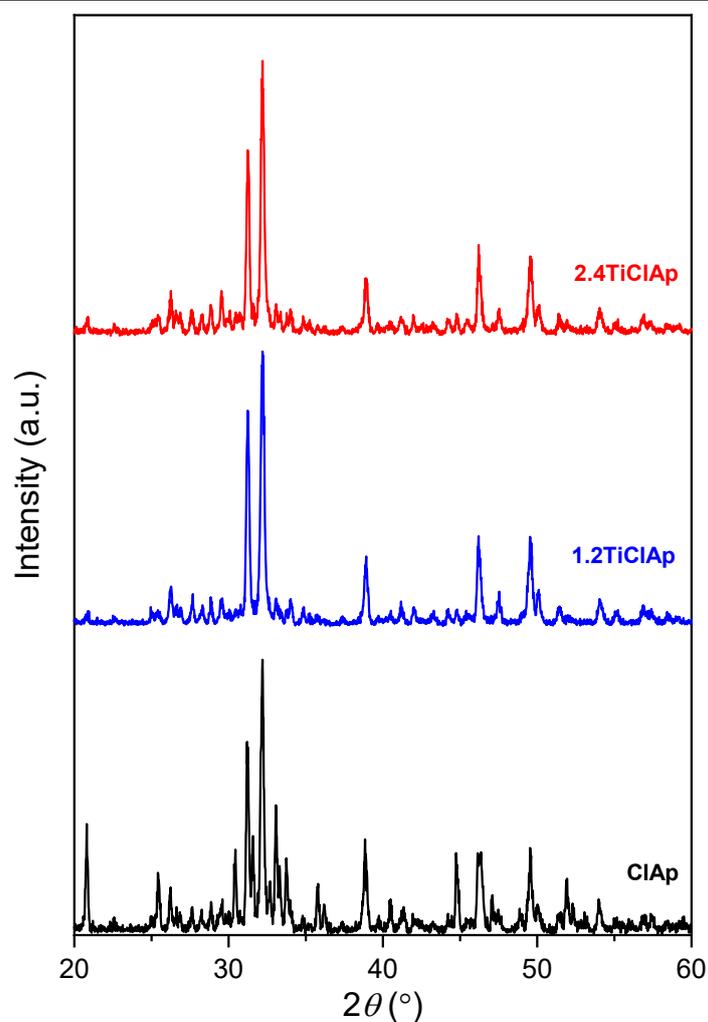
Fig. 5. XRD patterns of the un-doped and Ti-doped ClAp samples

4.2.2. FTIR measurement results

Fig. 6 shows the FTIR spectrum for each sample. The wide band at 3468 cm^{-1} and the narrow one at 1639 cm^{-1} are associated with the water [23]. The bands of 1053, 602 and 569 cm^{-1} are assigned to the phosphate group of the apatite structure [24, 25]. The band centered at 1385 cm^{-1} can be related to the carbonate group [25].
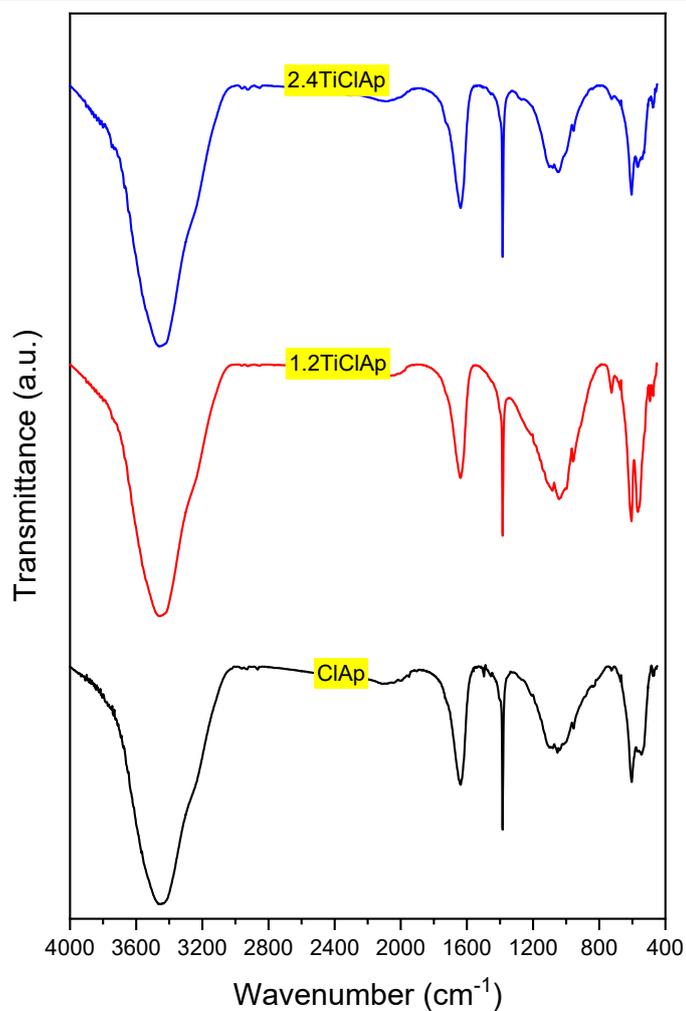
Fig. 6. FTIR spectra of the un-doped and Ti-doped ClAp samples

4.2.3. SEM observations

SEM images of the as-prepared ClAp samples taken at a voltage of 15 keV and magnification of X 2,000 are shown in Fig. 7. All the samples have almost the same morphology. The formation of the microplates, composed of smaller sphere-like particles, stacked on top of each other was observed for all the ClAp samples.
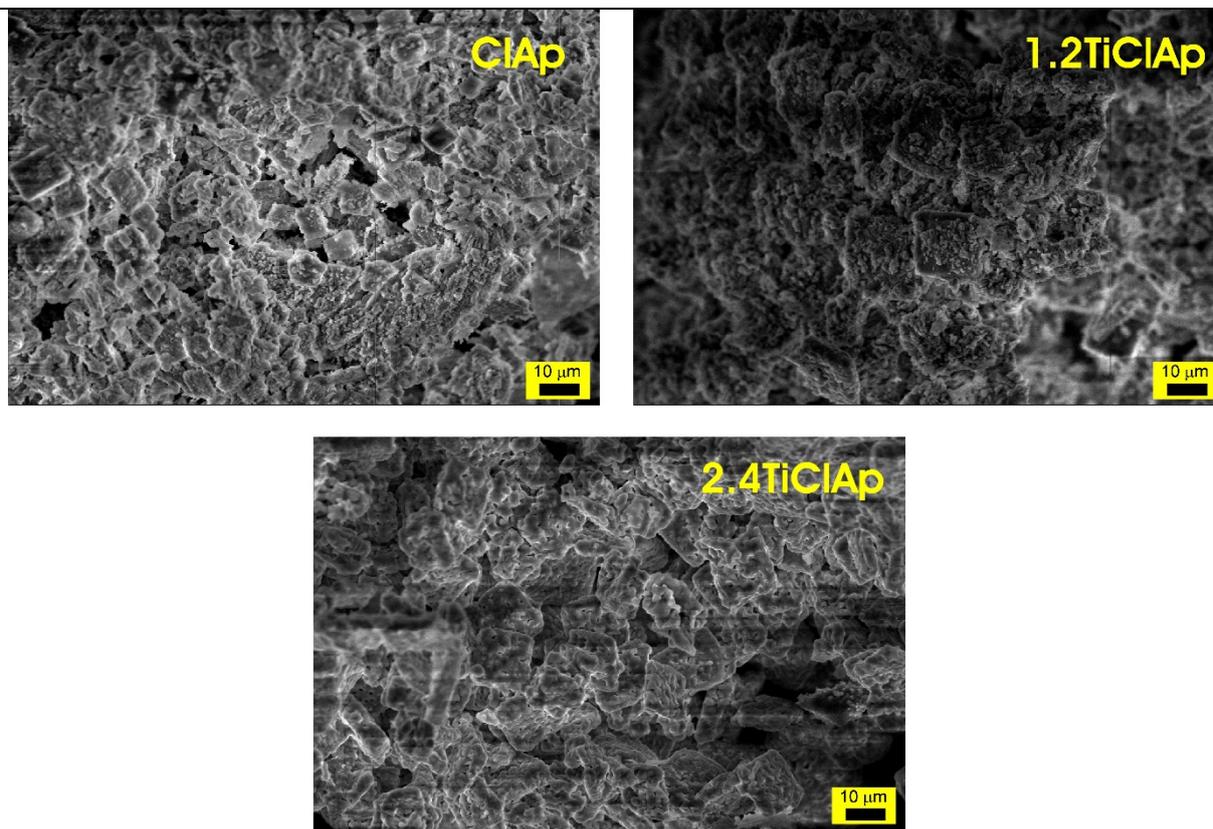
Fig. 7. SEM images of the un-doped and Ti-doped ClAp samples

5. Conclusion

The investigation into Ti-doped chlorapatite (ClAp) structures, conducted for the first time to the best of our knowledge, unveils valuable insights into the electronic and structural properties of these materials. The apatite family, encompassing compounds like ClAp, holds paramount significance in the realm of inorganic compounds due to their widespread occurrence in igneous rocks and their diverse elemental components. ClAp, with its hexagonal structure and space group $P6_3/m$, features distinct arrangements of divalent metal ions (MI and MII) surrounded by oxygen atoms and chloride ions, forming a network with phosphate ions. Our theoretical calculations elucidate the electronic band structure of un-doped ClAp, indicating an insulating nature with a calculated band gap of approximately 4.947 eV. The theoretical volume parameter closely aligns with experimental observations (0.5539 vs. 0.5638 nm^3), validating the accuracy of our computational model. Introducing titanium (Ti) as a dopant in 1.2TiClAp results in an increased band gap of about 5.339 eV, with excellent agreement between theoretical and experimental volume parameters (0.5538 and 0.5484 nm^3, respectively). For 2.4TiClAp, the band gap remains stable at approximately 5.344 eV, with the theoretical and experimental volume parameters of 0.5260 and 0.5430 nm^3. These systematic variations in band gaps with titanium doping underscore the tunability of electronic properties in Ti-doped ClAp, suggesting potential applications across various fields. The reliability of theoretical calculations is further evidenced by the consistent alignment between theoretical and experimental volume parameters. These findings contribute significantly to our fundamental understanding of the electronic behavior of Ti-doped ClAp, providing crucial insights for material design and optimization.

References

[1] A. Durugkar, S. Tamboli, N.S. Dhoble, S.J. Dhoble, "Novel photoluminescence properties of Eu^{3+} doped chlorapatite phosphor synthesized via sol-gel method" *Materials Research Bulletin*, 97, 466-472, 2018. https://doi.org/10.1016/j.materresbull.2017.09.043.

[2] H. Jena, B.K. Maji, R. Asuvathraman, K.V.G. Kutty, "Synthesis and thermal characterization of glass bonded Ca-chlorapatite matrices for pyrochemical chloride waste immobilization" *Journal of Non-Crystalline Solids*, 358, 1681-1686, 2012. https://doi.org/10.1016/j.jnoncrysol.2012.05.002.

[3] H. Jena, B.K. Maji, R. Asuvathraman, K.V.G. Kutty, "Effect of pyrochemical chloride waste loading on thermo-physical properties of borosilicate glass bonded Sr-chlorapatite composites" *Materials Chemistry and Physics*, 162, 188-196, 2015. http://dx.doi.org/10.1016/j.matchemphys.2015.05.057.

[4] N.J. Flora, K.W. Hamilton, R.W. Schaeffer, C.H. Yoder, "A Comparative Study of the Synthesis of Calcium, Strontium, Barium, Cadmium, and Lead Apatites in Aqueous Solution" *Synthesis and Reactivity in*

Inorganic and Metal-Organic Chemistry, 34(3), 503-521, 2004. https://doi.org/10.1081/SIM-120030437.

[5] B.K. Maji, H. Jena, R.V. Krishnan, R. Asuvathraman, K. Ananthasivan, K.V.G. Kutty, "Comparison of thermal expansion and heat capacity properties of various borosilicate glass-bonded strontium chlorapatite composites loaded with simulated pyrochemical waste" *Journal of Thermal Analysis and Calorimetry*, 119, 1825-1831, 2015. https://doi.org/10.1007/s10973-014-4322-1.

[6] H. Jena, R.V. Krishnan, R. Asuvathraman, K. Nagarajan, K.V.G. Kutty, "Thermal expansion and heat capacity measurements on Ba_{10-x} Cs $_x$ $(PO_4)_6Cl_{2-\delta}$, (x=0, 0.5) chlorapatites synthesized by sonochemical process" *Journal of Thermal Analysis and Calorimetry*, 106, 875-879, 2011. https://doi.org/10.1007/s10973-011-1715-2.

[7] M.H. Hwang, Y.J. Kim, S.H. Jung, S.H. Han, "Preparation and Luminescent Characterization of $M_5(PO_4)_3Cl$ (M: Sr, Ca) Chlorapatites by a Solid-state Reaction Method" *Synthesis and Reactivity in Inorganic and Metal-Organic Chemistry*, 38(3), 307-311, 2008. https://www.tandfonline.com/doi/full/10.1080/155331708 02023528.

[8] M. Ganjali, S. Pourhashem, M. Mozafari, "The effect of heat-treatment on the structural characteristics of nanocrystalline chlorapatite particles synthesized via an in situ wet-chemical route" *Ceramics International*, 41(10), 13100-13104, 2015, https://doi.org/10.1016/j.ceramint.2015.07.020.

[9] X. Xu, X. Yu, L. Mao, S.P. Yang, Z. Peng, "Preparation and photoluminescence of Bi^{3+}-doped strontium chlorapatite nano-phosphor" *Materials Letters*, 58(29), 3665-3668, 2004, https://doi.org/10.1016/j.matlet.2004.04.037.

[10] M. Nabiyouni, H. Zhou, S.B. Bhaduri, "Microwave assisted solution combustion synthesis (MASCS) of europium (Eu) doped chlorapatite nanowhiskers" *Materials Letters*, 108, 54-57, 2013, https://doi.org/10.1016/j.matlet.2013.06.089.

[11] R. Pazik, J.M. Nedelec, R.J. Wiglusz, "Preferential site substitution of Eu^{3+} ions in $Ca_{10}(PO_4)_6Cl_2$ nanoparticles obtained using a microwave stimulated wet chemistry technique" *CrystEngComm*, 16, 5308-5318, 2014, https://doi.org/10.1039/C4CE00197D.

[12] C.H. Wang, D.Y. Gui, R. Qin, F.L. Yang, X.P. Jing, G.S. Tian, W. Zhu, "Site and local structure of activator Eu^{2+} in phosphor $Ca_{10-x}(PO_4)_6Cl_2:xEu^{2+}$" *Journal of Solid State Chemistry*, 206, 69-74, 2013, https://doi.org/10.1016/j.jssc.2013.07.035.

[13] B. Nasiri-Tabrizi, W.J. Basirun, B. Pingguan-Murphy, "Mechanochemical preparation and structural characterization of Ta-doped chlorapatite nanopowders" *Progress in Natural Science*, 26(6), 546-554, 2016, https://doi.org/10.1016/j.pnsc.2016.11.010.

[14] B. Nasiri-Tabrizi, E. Zalnezhad, B. Pingguan-Murphy, W.J. Basirun, A.M.S. Hamouda, S. Baradaran, "Structural and morphological study of mechanochemically synthesized crystalline nanoneedles of Zr-doped carbonated chlorapatite" *Materials Letters*, 149, 100-104, 2015, https://doi.org/10.1016/j.matlet.2015.02.125.

[15] L. Wang, K. Liu, J. Wang, L. Zhao, Y. Xu, R. Zhou, L. Chen, B. Qu, "Defects levels and VUV/UV luminescence of Ce^{3+} and Eu^{3+} doped chlorapatite phosphors $M_5(PO_4)_3Cl$ (M = Ca, Sr, Ba)" *Optical Materials*, 107, 110014, 2020, https://doi.org/10.1016/j.optmat.2020.110014.

[16] Z. Zhang, J. Wang, M. Zhang, Q. Zhang, Q. Su, "The energy transfer from Eu^{2+} to Tb^{3+} in calcium chlorapatite phosphor and its potential application in LEDs" *Applied Physics B*, 91, 529-537, 2008, https://doi.org/10.1007/s00340-008-3035-1.

[17] Y.K. Kim, M. Lee, H.S. Yang, M.G. Ha, K.S. Hong, "Optical characteristics of the rare-earth-ions-doped calcium chlorapatite phosphors prepared by using the solid–state reaction method" *Current Applied Physics*, 16(3), 357-360, 2016, https://doi.org/10.1016/j.cap.2015.12.016.

[18] A. Fahami, G.W. Beall, "Mechanosynthesis of carbonate doped chlorapatite–ZnO nanocomposite with negative zeta potential" *Ceramics International*, 41(9), 12323-12330, 2015, https://doi.org/10.1016/j.ceramint.2015.06.061.

[19] S.J. Clark, M.D. Segall, C.J. Pickard, P.J. Hasnip, M.I.J. Probert, K. Refson, M.C. Payne, "First Principles Methods Using CASTEP" *Zeitschrift für Kristallographie-Crystalline Materials*, 220, 567-570, 2005, https://doi.org/10.1524/zkri.220.5.567.65075.

[20] K. Momma, F. Izumi, "VESTA 3 for three-dimensional visualization of crystal, volumetric and morphology data" *Journal of Applied Crystallography*, 44, 1272-1276, 2011, http://dx.doi.org/10.1107/S0021889811038970.

[21] C.C. Ribeiro, I. Gibson, M.A. Barbosa, "The uptake of titanium ions by hydroxyapatite particles-structural changes and possible mechanisms" *Biomaterials*, 27(9), 1749-1761, 2006, https://doi.org/10.1016/j.biomaterials.2005.09.043.

[22] B.D. Cullity, "Elements of X-ray diffraction" Addison-Wesley Publishing Company, Massachusetts, 1978

[23] M.E. Fleet, X. Liu, "Type A–B carbonate chlorapatite synthesized at high pressure" *Journal of Solid State Chemistry*, 181(9), 2494-2500, 2008, https://doi.org/10.1016/j.jssc.2008.06.016.

[24] L.D.A. Cavalcante, L.S. Ribeiro, M.L. Takeno, P.T.P. Aum, Y.K.P.G. Aum, J.C.S. Andrade, "Chlorapatite derived from fish scales" *Materials*, 13(5), 1129, 2020, https://doi.org/10.3390/ma13051129.

[25] A. Fahami, G.W. Beall, T. Betancourt, "Synthesis, bioactivity and zeta potential investigations of chlorine and fluorine substituted hydroxyapatite" *Materials Science and Engineering: C*, 59, 78-85, 2016, https://doi.org/10.1016/j.msec.2015.10.002.